In ovo application of antagomiRs indicates a role for miR-196 in patterning the chick axial skeleton through Hox gene regulation

Edwina McGlinn[a], Soraya Yekta[b,c], Jennifer H. Mansfield[a,1], Jürgen Soutschek[d], David P. Bartel[b,c], and Clifford J. Tabin[a,2]

[a]Department of Genetics, Harvard Medical School, 77 Avenue Louis Pasteur, Boston, MA 02115; [b]Whitehead Institute for Biomedical Research, 9 Cambridge Center, Cambridge, MA 02142; [c]Howard Hughes Medical Institute and Department of Biology, Massachusetts Institute of Technology, 77 Massachusetts Avenue, Cambridge, MA 02139; and [d]Regulus Therapeutics, 1896 Rutherford, Carlsbad, CA 92008

Patterning of the vertebrate axial skeleton requires precise spatial and temporal control of Hox gene expression during embryonic development. MicroRNAs (miRNAs) are recently described modulators of gene activity, and members of the miR-196 and miR-10 families have been shown to target several Hox genes in vivo. Testing miRNA function in mice is complicated by potential redundancy between family members. To circumvent this, we have developed protocols for introducing modified antisense oligonucleotides (antagomiRs) in ovo during chick development. Using this approach, we identify a layer of regulatory control provided by the miR-196 family in defining the boundary of Hox gene expression along the anterior-posterior (A-P) embryonic axis. Following knockdown of miR-196, we observe a homeotic transformation of the last cervical vertebrae toward a thoracic identity. This phenotypic alteration is, in part, due to an anterior expansion of Hoxb8 gene expression and consolidates the in vivo relevance of post-transcriptional Hox gene regulation provided by miRNAs in the complex hierarchies governing axial patterning.

axial patterning | microRNA | homeotic transformation

The distinct morphologies of vertebrae in different regions of the spine are essential to enable the axial skeleton to perform its structural and protective functions. Individual vertebra arise from a serially repeating unit, the somite, which itself is generated following sequential segmentation of a region of the caudal embryo known as the presomitic mesoderm (PSM). Although nascent somites appear morphologically homogenous regardless of A-P position, classic heterotopic grafting experiments indicate that all of the required information regarding their final A-P position is imparted at presegmentation stages (1). The nature of this positional information is thought to be largely a reflection of a cell's combinatorial Hox gene expression at a given axial level (2).

Hox genes are transcription factors orthologous to the HomC genes in Drosophila. When the function of these genes is altered, the insects exhibit striking alterations where one segment, or a part of a segment, develops with the morphology normally characteristic of a different segment. Such structural alterations are known as homeotic transformations (3, 4). Over the course of vertebrate evolution, a single ancestral HOM complex underwent duplication to produce four gene clusters, which when combined with gene loss within clusters resulted in the 39 Hox genes found in all extant mammals. Each cluster, HoxA through HoxD, contains 9–11 protein-coding genes dispersed among 13 paralogous groups. Within each cluster, all genes are transcribed in the same 5′-to-3′ orientation, allowing the clusters to be considered as having a 5′ and a 3′ end. This unique chromosomal organization facilitates coordination of Hox-cluster expression, such that genes located at the 3′ end of the cluster are expressed more anteriorly and earlier, whereas genes more 5′ are expressed progressively more posteriorly and at later stages of development (5, 6). This temporal and spatial colinearity of Hox gene expression, when coupled to a steady rate of PSM expansion and segmentation, establishes a staggered yet overlapping arrangement of Hox gene expression along the A-P axis.

A little-discussed but important aspect of this mechanism to consider is that it is initially not very robust. The spatial domains of Hox expression established during PSM segmentation do not precisely align with the somite boundaries and, moreover, at the edges of the Hox gene expression domains, gene activity is graded rather than being sharply delineated. This implies that there must be additional regulatory mechanisms to reproducibly achieve accurate regional identities. Indeed, in addition to global and local cis-regulatory elements, which drive colinear Hox expression, other layers of control are known to exist to regulate the final Hox protein output of a cell, however, they remain poorly defined. An important class of regulatory molecules that could potentially serve to sharpen and align Hox expression domains in the developing axial tissue is the miRNAs.

miRNAs are approximately 23 nucleotide RNA species that bind to even shorter complementary sequences generally in the 3′UTR of protein-coding transcripts to negatively regulate their expression (reviewed in ref. 7). In some cases, miRNAs appear to function to reinforce developmental decisions, dampening inappropriate expression of mRNAs in tissues where they do not belong, rather than as primary determinants of gene activity or cell fate (8–12); reviewed in (13). Intriguingly, two miRNA gene families are present, each with several members, within the Hox clusters themselves, and moreover have been shown to target multiple Hox genes. mir-10a and mir-10b lie upstream of Hox4 paralogs, and their genomic position and sequence is conserved in the Drosophila Hom complex (14). The mir-196 family members, of which there are three, lie upstream of Hox9 paralogs in the A, B, and C clusters (15). Although mir-196 appears only in vertebrate lineages, a distinct miRNA, mir-iab-4, is present at the syntenic region in Drosophila and targets the more 3′ gene Ubx with miRNAs produced from both DNA strands (15–19). Both of these miRNA families target multiple Hox genes, however, there is a bias such that the majority of their targets are genes located more 3′ in the cluster than themselves (15, 20–22). Thus expression of miRNAs encoded at a particular locus within a Hox cluster will limit activity of Hox genes 3′ to that locus, while leaving intact the activity of Hox genes lying 5′ to that locus. This, in principle, could serve to reinforce the general phenomenon
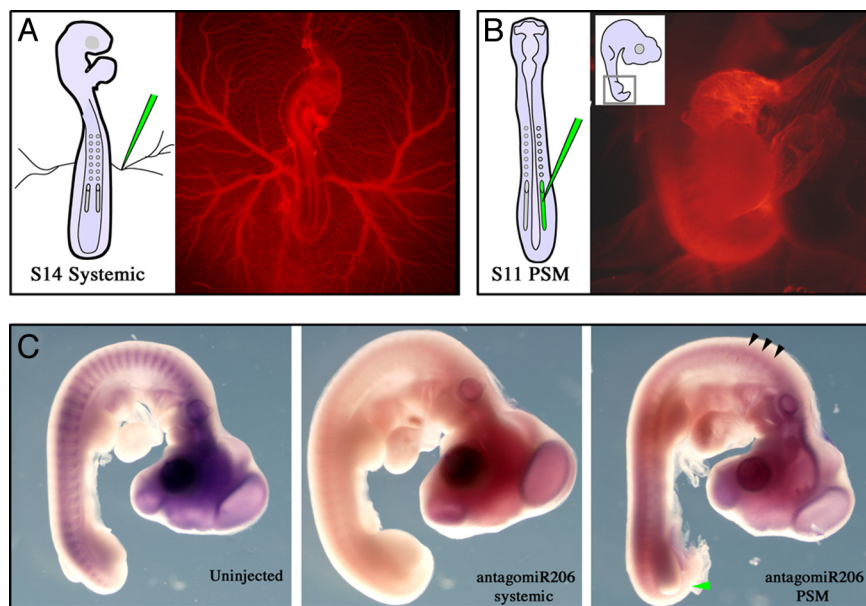
Fig. 1. AntagomiR knockdown of chick miRNAs *in ovo*. (*A*) Systemic delivery of antagomiRs was achieved as schematized by injection into the vitteline vein of a S14–S18 chicken embryo. Tracing of flurophore-conjugated antagomiR indicates rapid dispersal throughout the circulation by this delivery method, shown here 10 min post injection. (*B*) Localized delivery of antagomiR targeting precursors of the axial skeleton was achieved as schematized by injection into the presomitic mesoderm (PSM) of stage 11 chick embryos. High level flourophore-conjugated antagomiR was observed with a strong caudal bias 27 h post injection. (*C*) Efficacy of miRNA knockdown as assessed by in situ hybridization 2 days following injection of antagomiR206. Strong myotomal expression of miR-206 observed in uninjected embryos was either completely abolished or greatly downregulated when antagomiR206 was injected systemically or into the PSM respectively. For PSM injected embryos, green arrow head indicates site of injection while black arrow heads indicate sustained miR-206 expression in anterior-most somites.

known a "posterior prevalence," the phenotypic dominance of 5′ Hox genes over 3′ Hox genes coexpressed in the same cell (21).

Although targets of miR-10 and miR-196 have been predicted *in silico*, and in some cases experimentally supported in vitro, loss-of-function studies to address the in vivo relevance of these interactions is complicated due to the potential redundancy between different miRNA family members. Each of these two miRNA families shares near identical sequence and the same predicted targets. Moreover, each paralogue of *mir-10* and of *mir-196* lies in an equivalent location within their respective Hox clusters, and are likely regulated spatially and temporally like the adjacent Hox genes (20). Thus genetically determining the function of the Hox-embedded miRNAs in mice would potentially require constructing double or triple knockouts. To circumvent this issue and get at least an initial indication of the in vivo role of the Hox-embedded miRNAs in higher vertebrates, we turned to a knockdown strategy.

A modified antisense oligonucleotide technology (antagomiRs) has been described that is capable of efficiently and irreversibly knocking down miRNA function when applied systemically in adult mice (23). With its embryonic accessibility, the chick system offers an attractive setting in which to test the developmental roles of individual miRNA families. We find that, indeed, antagomiRs can be delivered either locally or systemically into the developing chicken embryo and result in the knockdown of endogenous miRNA expression.

The development of this in vivo system has allowed us to simultaneously knock down all three miR-196 paralogs. Knockdown of miR-196 function in the early embryo resulted in a homeotic transformation of the last cervical vertebra toward a thoracic identity, concomitant with an anterior expansion of *HoxB8* expression. These data place miRNA regulation of Hox gene expression as an integral component of the gene networks governing chick axial patterning. Moreover, the success of this

approach provides a framework for designing high-throughput analyses of miRNA function in developing vertebrate embryos.

Results

AntagomiR Knockdown of Chick miRNAs *in Ovo*. To understand the in vivo roles of the Hox-embedded miRNAs during embryonic development in higher vertebrates we wanted to adopt the use of antagomiRs, modified antisense oligonucleotides previously shown to knock down levels of miRNAs in adult mouse (23). Due to its accessibility, we reasoned that the chicken embryo might be a context where these reagents could be readily used. First, to assess efficiency of delivery methods, we monitored the distribution of a fluorescently labeled 5′-Cy3-antagomiR following injection *in ovo*. For this analysis we used a control antagomiR complementary to miR-122, a liver-specific miRNA that would not be predicted to disrupt early developmental functions. Fluorescence signal was detected immediately throughout the circulatory system following injection into the extra-embryonic vitelline vein of stage-14–18 chick embryos (Fig. 1*A*). Weak signal could be observed within the embryo proper up to 27 h post injection. Given our interest in targeting progenitors of the axial skeleton, we also attempted a more localized method of antagomiR delivery, directly into the presomitic mesoderm of stage 11–12 embryos (Fig. 1*B*). High-level fluorescent signal could be observed extending beyond the injection site, although with a clear caudal bias at 27 h post injection (Fig. 1*B*) and maintained up to at least 44 h. Stability of fluorescence conjugation to the antagomiR has been assessed in other in vivo settings and fluorescence signal shown to correlate to active antagomiR function (24).

To establish the general applicability of the approach we wanted to judge the ability of antagomiRs to appreciably knock down levels of even relatively highly expressed miRNAs. We therefore chose to assess miR-206, which exhibits high expression in the somitic subcompartment the myotome (25) and whose
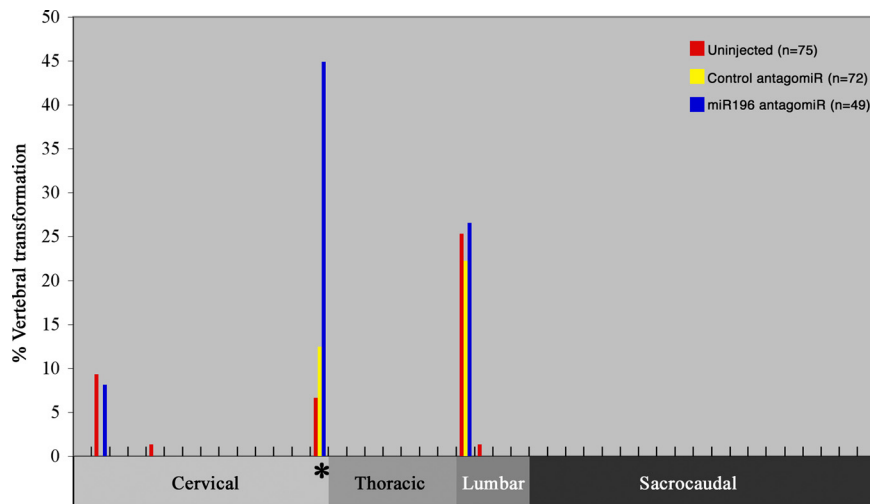
Fig. 2. Homeotic transformations of the axial skeleton observed following PSM antagomiR196 injection. Homeotic transformations observed for each individual vertebral segment, expressed as a percentage of total embryo number for each condition. The asterisk represents statistical significance (P value <0.05) of the frequency of defects at a given position, calculated by Fisher's Exact Test.

distinctive striped spatial distribution can be easily detected by whole-mount in situ hybridization using locked nucleic acid (LNA) riboprobes (26). Embryos were injected either systemically or directly into the PSM as above, and assessed for miRNA expression 2 days post injection (stage 21–22) (Fig. 1C). Strong myotomal expression of miR-206 in uninjected embryos was no longer detected following systemic injection of antagomiR206 ($n = 5/5$). A significant reduction also was observed following PSM injection ($n = 5/5$), although the loss of detectable miR-206 expression was highest near the site of injection (green arrow head) and faint striped miR-206 expression could still be detected in the anterior-most somites (black arrow heads). Together, these data suggest that antagomiR-based technology could be adapted to provide a rapid and efficient method for assessing developmental roles of individual miRNA families in the chick. These results encouraged us to use the method to examine the in vivo role of miR-196.

Knockdown of miR-196 *in Ovo* Results in Vertebral Transformations at the Cervical-Thoracic Boundary. To assess a potential role for miR-196 in patterning of the axial skeleton, we knocked down miRNA levels via localized delivery of antagomiR196 into the PSM. This method was chosen because it allowed unilateral treatment and hence direct comparison of skeletal morphology on the left and right sides of the embryo. The three chick miR-196 genes share 100% sequence similarity across the entire mature miRNA, and thus our antagomiR approach will simultaneously knock down all miR-196 species.

Embryos were unilaterally injected in the PSM with a single dose of antagomiR196 or a control antagomiR122 at stage 11–12 of development, a timepoint correlating to generation of mid-cervical (prevertebrae pv8), and more caudal vertebrae. Day 11 skeletons were assessed for deviations from a wild-type axial body pattern of 14 cervical, 7 thoracic, 4 lumbar, and up to 19 sacrocaudal vertebrae. Phenotypic variation of individual vertebra and vertebral identity was assessed on the basis of the shape of the vertebral body and the presence or absence of a rib. Vertebral identities were compared to the standard avian axial formula, and deviations were scored as transformations. In addition, malformations were recorded, such as unfused vertebrae, hemivertebrae or missing processes.

A highly significant posteriorizing transformation of the last cervical vertebra (C14) was observed in antagomiR196-treated embryos (p value, 0.0001) (Fig. 2). The presence of an ectopic rib

at C14 was observed in 22/49 (45%) of antagomiR196 embryos, which was higher than that observed in either uninjected (5/75; 7%), or control-antagomiR-injected (9/72; 12.5%) embryos (Figs. 2 and 3C). Low-level variation in the axial formulae between wild-type individuals has been observed previously (27), and we observed this particularly at both thoracic transition points (Fig. 2). However, the low-frequency C14 transformations observed in uninjected or control-injected embryos almost always consisted of very short bilateral unossified cartilaginous elements. In contrast, the majority of C14 transformations in antagomiR196-injected embryos were unilateral, on the injected (right-hand) side of the embryo, and consisted of a large rib process that was beginning to ossify as indicated by the presence of alizarin red (Fig. 3A). Unilateral left-hand side ectopic C14 ribs were never observed. In addition, we observed posteriorizing transformations at C2, with the appearance of C3- and C4-specific foramina. However these occurred at a frequency similar to that seen in uninjected/control embryos, suggesting that this alteration reflected natural variation.

We also analyzed the occurrence of vertebral transformations following systemic knockdown of miR-196 by a single dose of antagomiR196 injected through the vitelline vein at stage 14–18. The same trend of increased C14 to thoracic transformation was observed as seen with the localized injections (Fig. S1), although given the number of injections performed the deviation from wild type did not reach statistical significance. Systemic injections were not pursued further as no additional phenotypes were observed by this approach, and because unilateral effects could not be used to help parse out induced transformations from natural variation.

Decrease in miR-196 Activity *in Ovo* Results in Upregulation of Predicted Target Gene Expression. According to current predictions, the miR-196 family may target at least nine Hox genes in chick (*Hoxb1, Hoxa5, Hoxb6, Hoxa7, Hoxb7, Hoxb8, Hoxc8, Hoxa9,* and *Hoxb9*) (21, 28), and a number of these have been supported experimentally (10, 15, 20). In most vertebrates, *Hoxb8* has extensive complementarity to the miRNA, which leads to mRNA cleavage in the center of the site (15). Although in chick this extensive complementarity has been replaced by a more typical seed-pairing interaction, *Hoxb8* mRNA degradation following miR-196 overexpression has been demonstrated (10). We therefore assessed the mRNA localization of *Hoxb8* in chick 4–6 h following antagomiR injection. We observed a shift
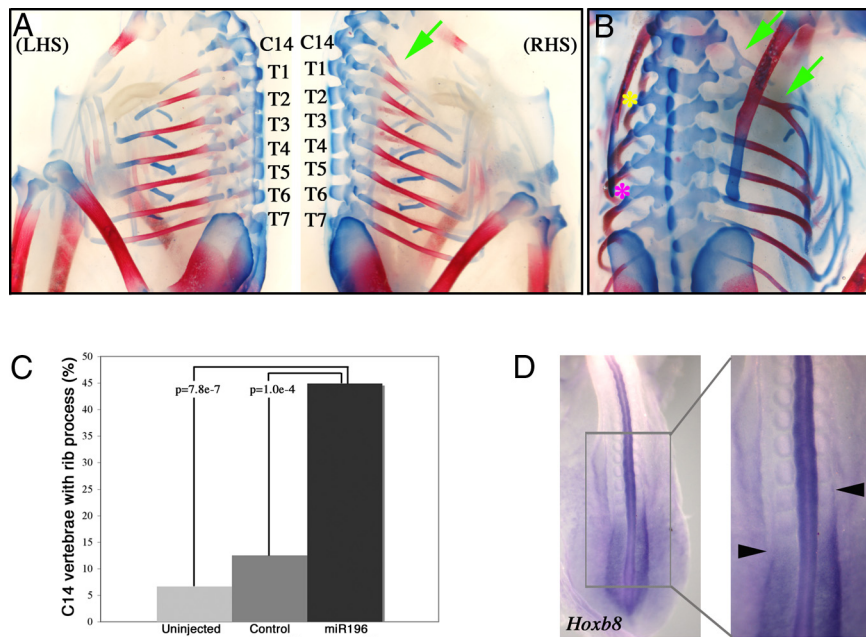
Fig. 3. Knockdown of miR-196 within the PSM induces cervical to thoracic homeotic transformations in chick. (*A*) Skeletal analysis of antagomiR196 injected embryos reveals an additional rib-like process on the 14th cervical vertebrae (green arrow). This additional rib was often unilateral, present on the injected right-hand side (RHS) when compared to the uninjected left-hand side (LHS). (*B*) Other common axial skeletal defects observed include split vertebrae (yellow asterix), hemivertebrae (pink asterix) and fused proximal ribs (green arrows). (*C*) Analysis using Fisher's test indicates a statistically significant increase in the number of C14 vertebrae with rib like process in antagomiR196 injected embryos when compared to control injected or uninjected embryos. (*D*) Interrogation of *Hoxb8* mRNA levels in antagomiR196 injected embryos reveals an expansion of the anterior limit *Hoxb8* on the injected side.

in the anterior boundary of *Hoxb8* on the injected (right-hand) side of the embryo ($n = 8/15$) (Fig. 3*D*). Moreover, the anterior boundary appeared more graded in these cases, with a less abrupt transition from *Hoxb8*-expressing to *Hoxb8*-nonexpressing somites (Fig. 3*D*). This anterior shift of approximately 1–3 somites correlates well with the anterior extent and unilateral nature of the observed phenotype. It is highly likely that the phenotype results from a combined derepression of multiple Hox transcripts, including *Hoxb6*, *Hoxa7*, and *Hoxb7* in addition to *Hoxb8*.

AntagomiR Injection Results in Vertebral Malformation. In addition to homeotic transformations, numerous malformations of ver-

tebral elements were observed following PSM-injection of either antagomiR196 or control antagomiR (Fig. 4). These malformations included defects in both vertebral segmentation and formation, ranging from minor alterations in transverse process morphology to more severe cases of split vertebrae, hemivertebrae and vertebral fusions (Fig. 3*B*). We also observed numerous alterations in rib formation such as fused (Fig. 3*B*) or absent ribs. With the possible exception of C6 vertebrae, no significant difference in vertebral malformation number was observed across the axial skeleton when comparing antagomiR196- and control antagomiR-treated embryos, suggesting such malformations are a nonspecific consequence of PSM antagomiR treat-
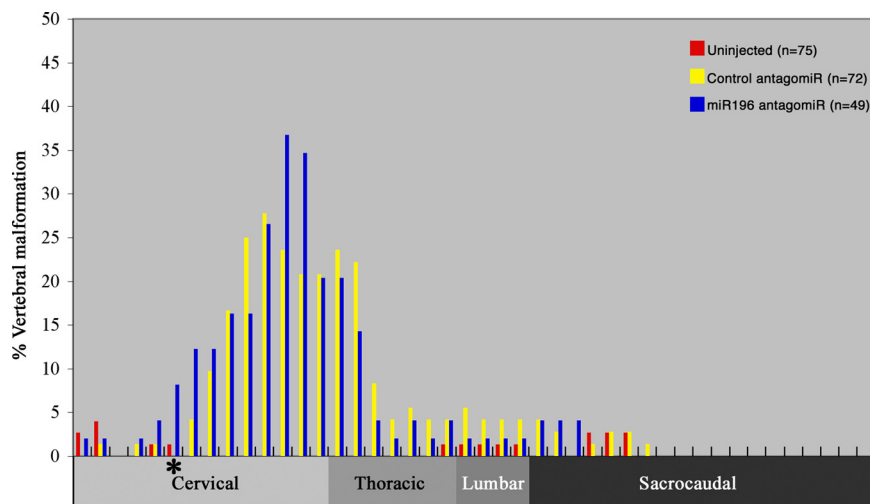
Fig. 4. Presomitic mesoderm antagomiR injection induces skeletal malformations. Vertebral malformations observed for each individual segment, expressed as a percentage of total embryo number for each condition. The asterisk represents statistical significance (P value <0.05) of the frequency of defects at a given position, calculated by Fisher's Exact Test.

ment. Nonetheless, analysis of vertebral malformations following systemic antagomiR delivery indicated a statistically significant increase of antagomiR196-induced malformation of 10 vertebral segments, suggesting a role for miR-196 in later aspects of vertebrae differentiation (Fig. S1). The discrepancy observed between alternate injection techniques will await clarification following complete genetic removal of miR-196 in mouse.

Discussion

We demonstrate here the *in ovo* application of antagomiRs to successfully knock down miRNA function in chick embryos. Using this technique we have uncovered a role for miR-196 in refining the anterior extent of somitic *Hoxb8* expression and consequently, in appropriate regionalization of the axial skeleton.

In Ovo Knockdown of miRNAs Using AntagomiRs.
Knockdown of miRNA function, revealing a proneurogenic role for miR-124 in the early chicken embryo, has previously been achieved following electroporation of either LNA-stabilized (29) or 2′-0-methyl modified (30) antisense oligos into the developing neural tube. This delivery method however is not suited to many embryonic contexts. The success of systemic antagomiR delivery in mouse for knocking down miRNA expression across a wide range of adult tissues (23) prompted us to trial this technology, and indeed, we show a dramatic reduction in miRNA detection following systemic or more localized delivery in chick embryos (Fig. 1). It is possible that the observed reduction in miR-206 detection following antagomiR treatment represented either miRNA degradation (31) or competitive inhibition of in situ detection by sustained presence of the antisense antagomiR (32), or likely, a combination of both scenarios. However, even in the latter case, the continued presence of the antagomiR would likely allow it to interfere with binding to its target, just as it masks the microRNA from the hybridization probe. Moreover, our functional analysis strongly suggests that the loss of miRNA signal in the in situ hybridization correlates with a loss of miRNA activity in vivo. The methods described here coupled with the wealth of information currently being generated from deep sequencing and in situ hybridization screens detailing tissue-specific miRNA expression in chick (25, 33, 34) will enable rapid functional assessment of individual miRNAs during development. These approaches will complement lengthier knockout approaches in mouse, or may help elucidate species-specific miRNA functions given the observation of miRNAs unique to the avian lineage (34), as well as the divergence of some miRNA expression patterns between species (35).

miR-196 Regulates Hox Expression and Vertebral Identity.
Given the widespread predicted regulation of Hox genes by miR-196, we have focused our knockdown studies on addressing the role of this miRNA family in patterning the axial skeleton. Many of the Hox genes predicted to be targets of miR-196 are known to influence vertebral identity at the thoracic level; however interpretation of the Hox code at this axial level is not straightforward. Analogous to homeotic phenotypes in fly, loss of Hox function often results in anterior transformations while gain of Hox function into more anterior domains leads to a posteriorizing effect. Contrary to these general trends, Hoxa5, a target of miR-196 in chick, exhibits posteriorization upon loss of function (36) suggesting derepression of this gene is unlikely to contribute to the observed phenotype following miR-196 loss-of-function. Conversely, a T1 to C7 transformation is observed in *Hoxa6* single and *Hoxa7;Hoxb7* double mutant embryos (37, 38). These genes are predicted targets of miR-196, *Hoxa7* harboring up to five conserved 8-mer binding sites for this miRNA family (21). The sufficiency of these Hox genes to posteriorize when ectopically expressed in a more anterior location has been tested at

least for Hoxb7, and indeed, ectopic rib formation was observed on the last cervical vertebrae (39). Similar extension of the anterior boundary of Hoxb8 led to dramatic homeotic transformations, with ectopic ribs observed on up to five cervical vertebrae (40). Our observation that loss of miR-196 leads to a derepression of *Hoxb8* expression in more anterior somites thus provides at least partial mechanistic insight into the observed phenotype.

Mechanism of Regulation of Hox Targets by miR-196.
With such extensive predicted Hox gene regulation, it is somewhat surprising that the phenotype we observe is relatively subtle. While this may be a reflection of the transient knockdown approach, it does fit well with increasing data across many species that miRNAs themselves sometimes do not drive cell fate specification, but rather, act to fine tune or reinforce genetic pathways during development (8, 9, 12, 13). In considering this, it is important to address the degree of coexpression between a miRNA and its targets. The expression domain of miR-196, while broadly conforming to Hox cluster constraints (20) is yet to be precisely defined. Its positioning between Hox9 and 10 paralogs along with the overlapping nature of axial Hox gene expression suggests miR-196 will be, perhaps to a large extent, coexpressed with its target Hox transcripts. In addition to this, the location of miR-196 paralogs more 5′ in the cluster than any of its target hox genes (21) would predict that miR-196 expression will extend more posteriorly, and at this location may prevent aberrant posterior expansion of these target genes ("fail-safe" interaction). In support of a fail-safe interaction, miR-196 is known to prevent spurious *Hoxb8* expression in the developing vertebrate hindlimb (10). In *Drosophila*, miR-iab-4 exhibits a largely reciprocal pattern of expression with its target *Ubx*, although some areas of overlap do exist (16). Loss of miR-iab-4 function yields a subtle posterior expansion of *Ubx* expression in the nerve cord (19), consistent with our own subtle phenotype. The lack of posterior axial defects does not rule out a role for miR-196 in shaping the posterior limit of target Hox gene expression. It is possible that, given the early stage of our injections, by the time more caudal axial progenitors are being specified the level of antagomiR has been titrated to subphenotypic levels or that in this context, the action of more 5′ Hox genes prevail over ectopically expressed 3′ Hox gene expression.

Our experiments would suggest; however, that miR-196 acts to refine the anterior boundary of Hox target gene expression. miR-196 expression within precursors of vertebrae at the cervical-thoracic transition is likely given that murine *Hoxb9*, to which *mir-196a-1* is tightly associated genomically, is expressed very early in development with an anterior limit of pv3, and that murine loss-of-function phenotypes for *Hoxa9;Hoxb9* affect T1 and T2 rib process morphology (41). In addition, all three miR-196 genes in mouse have been identified as part of longer multigene transcripts, in each case cotranscribed with more anterior Hox genes one of which is a known miR-196 target (42).

The question therefore arises, why is miR-196 function opposing Hox transcriptional output at the anterior boundary of target gene expression? While each vertebrae is unique, the transition from one vertebral subtype to another involves a significant switch in the quantitative and qualitative Hox code (27). Even though robust, the *cis*-acting elements driving colinear Hox expression do not act at high enough resolution to eliminate all fluctuations in the system, as indicated by low level variation in axial formulae (Fig. 2). Fluctuations in Hox expression level would be most apparent when a gene is at low levels within the cell, for example, when expression is initiated. The coexpression of miR-196 would dampen protein output of its Hox target genes, thereby setting higher the threshold of transcriptional output needed to influence vertebral identity. This higher threshold might be achieved more reliably than would a

lower one because it would not be subject to the stochastic fluctuations associated with a fewer number of transcripts (43, 44). In this way miR-196 could be a key component of a system that specifies the crisp transition between nonrib-bearing cervical and rib-bearing thoracic vertebrae.

Materials and Methods

Embryo Manipulation. Chick eggs (SPAFAS) were incubated at 38 °C and staged according to (45). Systemic administration of antagomiRs was achieved by injection into the extra-embryonic vitelline vein of stage 14–18 chicken embryo. Localized administration of antagomiRs was achieved by injection into the presomitic mesoderm of stage 11–12 chick embryos. Following injection, embryos were reincubated until day 10–11 and then processed for skeletal staining as previously described (46).

Analysis of Skeletal Phenotypes. Skeletons were assessed for deviations from a wildtype axial body pattern of 14 cervical (C1–C14), 7 thoracic (T1–T7), 4 lumbar (L1–L4) and up to 19 sacrocaudal (S1–Cn) vertebrae. Phenotypic variation of individual vertebra was scored as either a transformation or a malformation. Unilateral, bilateral, partial, or complete homeotic transformations were grouped together and counted equally in the scoring. Abnormalities that could not clearly be recognized as a transformation were counted as malformations. Deletions of caudal (coccygeal) vertebrae were treated separately as a single malformation rather than malformation of each missing segment. P-values for the significance of the frequency of defects at each vertebral segment between experimental and control treatments were obtained by Fisher's Exact test.

AntagomiR Synthesis. AntagomiRs are 3′-cholesteryl-conjugated ribonucleic acids with the following stabilizing backbone chemical modifications: 2′-methoxy groups throughout, and phosphorothioates substituting three 3′-terminal and two 5′-terminal phosphodiester linkages. Oligonucleotides with sequences complementary to mature miRNAs were synthesized and RP-HPLC-purified (Regulus or Dharmacon), dissolved in water, and injected at 2 mg/mL (PSM injection) or 4.5 mg/mL (systemic injection) in sterile phosphate buffer saline. PSM injection has the advantage of higher local concentration of antagomiR within axial precursors resulting in a high efficiency of vertebral transformations, however, nonspecific vertebral malformations were observed. Systemic injection of approximately equivalent antagomiR concentration overcame this issue of nonspecific malformations, however diffusion throughout the circulation resulted in a reduced efficiency of specific phenotypic alterations. Three separate controls were tested in these experiments (antagomiR122, antagomiR375, and antagomiR223) and were chosen based on the restricted expression profiles of their target miRNAs to the liver (miR-122), pancreatic islet cells (miR-375), and myeloid lineage of the heamatopoietic system (miR-223). As such, we would predict these antaogomiRs will not influence patterning of the axial skeleton and consistent with this, C14 transformations were not observed following injection of any individual control antagomiR. For systemic injections, data were obtained using both antagomiR375 and antagomiR223, and the data for antagomiR375 is presented given the most injections were performed for this control.

AntagomiR196 5′-CCAACAACAUGAAACUACCUA; Presomitic mesoderm injection control (antagomiR122) 5′-ACAAACACCAUUGUCACACUCCA; Systemic injection control (antagomiR375) 5′ UAACGCGAGCCGAACGAACAAA; antagomiR206 5′-CCACACACUUCCUUACAUUCCA.

1. Kieny M, Mauger A, Sengel P (1972) Early regionalization of somitic mesoderm as studied by the development of axial skeleton of the chick embryo. *Dev Biol* 28:142–161.
2. Kessel M, Gruss P (1991) Homeotic transformations of murine vertebrae and concomitant alteration of Hox codes induced by retinoic acid. *Cell* 67:89–104.
3. Lewis EB (1963) Genes and developmental pathways. *Am Zool* 3:33–56.
4. Lewis EB (1978) A gene complex controlling segmentation in Drosophila. *Nature* 276:565–570.
5. Duboule D, Dolle P (1989) The structural and functional organization of the murine HOX gene family resembles that of Drosophila homeotic genes. *EMBO J* 8:1497–1505.
6. Graham A, Papalopulu N, Krumlauf R (1989) The murine and Drosophila homeobox gene complexes have common features of organization and expression. *Cell* 57:367–378.
7. Bartel DP (2009) MicroRNAs: Target recognition and regulatory functions. *Cell* 136:215–233.
8. Stark A, Brennecke J, Bushati N, Russell RB, Cohen SM (2005) Animal MicroRNAs confer robustness to gene expression and have a significant impact on 3′UTR evolution. *Cell* 123:1133–1146.
9. Li X, Cassidy JJ, Reinke CA, Fischboeck S, Carthew RW (2009) A microRNA imparts robustness against environmental fluctuation during development. *Cell* 137:273–282.
10. Hornstein E, et al. (2005) The microRNA miR-196 acts upstream of Hoxb8 and Shh in limb development. *Nature* 438:671–674.
11. Yi R, et al. (2006) Morphogenesis in skin is governed by discrete sets of differentially expressed microRNAs. *Nat Genet* 38:356–362.
12. Giraldez AJ, et al. (2005) MicroRNAs regulate brain morphogenesis in zebrafish. *Science* 308:833–838.
13. Hornstein E, Shomron N (2006) Canalization of development by microRNAs. *Nat Genet* 38 Suppl:S20–24.
14. Lagos-Quintana M, Rauhut R, Meyer J, Borkhardt A, Tuschl T (2003) New microRNAs from mouse and human. *RNA* 9:175–179.
15. Yekta S, Shih IH, Bartel DP (2004) MicroRNA-directed cleavage of HOXB8 mRNA. *Science* 304:594–596.
16. Ronshaugen M, Biemar F, Piel J, Levine M, Lai EC (2005) The Drosophila microRNA iab-4 causes a dominant homeotic transformation of halteres to wings. *Genes Dev* 19:2947–2952.
17. Stark A, et al. (2008) A single Hox locus in Drosophila produces functional microRNAs from opposite DNA strands. *Genes Dev* 22:8–13.
18. Tyler DM, et al. (2008) Functionally distinct regulatory RNAs generated by bidirectional transcription and processing of microRNA loci. *Genes Dev* 22:26–36.
19. Bender W (2008) MicroRNAs in the Drosophila bithorax complex. *Genes Dev* 22:14–19.
20. Mansfield JH, et al. (2004) MicroRNA-responsive 'sensor' transgenes uncover Hox-like and other developmentally regulated patterns of vertebrate microRNA expression. *Nat Genet* 36:1079–1083.
21. Yekta S, Tabin CJ, Bartel DP (2008) MicroRNAs in the Hox network: An apparent link to posterior prevalence. *Nat Rev Genet* 9:789–796.
22. Woltering JM, Durston AJ (2008) MiR-10 represses HoxB1a and HoxB3a in zebrafish. *PLoS ONE* 3:e1396.
23. Krutzfeldt J, et al. (2005) Silencing of microRNAs in vivo with 'antagomirs'. *Nature* 438:685–689.
24. Li QJ, et al. (2007) miR-181a is an intrinsic modulator of T cell sensitivity and selection. *Cell* 129:147–161.
25. Rathjen T, et al. (2009) High throughput sequencing of microRNAs in chicken somites. *FEBS Lett* 583:1422–1426.
26. Sweetman D, et al. (2006) FGF-4 signaling is involved in mir-206 expression in developing somites of chicken embryos. *Dev Dyn* 235:2185–2191.
27. Burke AC, Nelson CE, Morgan BA, Tabin C (1995) Hox genes and the evolution of vertebrate axial morphology. *Development* 121:333–346.
28. Grimson A, et al. (2007) MicroRNA targeting specificity in mammals: Determinants beyond seed pairing. *Mol Cell* 27:91–105.
29. Cao X, Pfaff SL, Gage FH (2007) A functional study of miR-124 in the developing neural tube. *Genes Dev* 21:531–536.
30. Visvanathan J, Lee S, Lee B, Lee JW, Lee SK (2007) The microRNA miR-124 antagonizes the anti-neural REST/SCP1 pathway during embryonic CNS development. *Genes Dev* 21:744–749.
31. Krutzfeldt J, et al. (2007) Specificity, duplex degradation, and subcellular localization of antagomirs. *Nucleic Acids Res* 35:2885–2892.
32. Davis S, et al. (2009) Potent inhibition of microRNA in vivo without degradation. *Nucleic Acids Res* 37:70–77.
33. Darnell DK, et al. (2006) MicroRNA expression during chick embryo development. *Dev Dyn* 235:3156–3165.
34. Glazov EA, et al. (2008) A microRNA catalog of the developing chicken embryo identified by a deep sequencing approach. *Genome Res* 18:957–964.
35. Ason B, et al. (2006) Differences in vertebrate microRNA expression. *Proc Natl Acad Sci USA* 103:14385–14389.
36. Jeannotte L, Lemieux M, Charron J, Poirier F, Robertson EJ (1993) Specification of axial identity in the mouse: Role of the Hoxa-5 (Hox1.3) gene. *Genes Dev* 7:2085–2096.
37. Chen F, Greer J, Capecchi MR (1998) Analysis of Hoxa7/Hoxb7 mutants suggests periodicity in the generation of the different sets of vertebrae. *Mech Dev* 77:49–57.
38. Rancourt DE, Tsuzuki T, Capecchi MR (1995) Genetic interaction between hoxb-5 and hoxb-6 is revealed by nonallelic noncomplementation. *Genes Dev* 9:108–122.
39. McLain K, Schreiner C, Yager KL, Stock JL, Potter SS (1992) Ectopic expression of Hox-2.3 induces craniofacial and skeletal malformations in transgenic mice. *Mech Dev* 39:3–16.
40. Charite J, de Graaff W, Deschamps J (1995) Specification of multiple vertebral identities by ectopically expressed Hoxb-8. *Dev Dyn* 204:13–21.
41. Chen F, Capecchi MR (1997) Targeted mutations in hoxa-9 and hoxb-9 reveal synergistic interactions. *Dev Biol* 181:186–196.
42. Mainguy G, Koster J, Woltering J, Jansen H, Durston A (2007) A Extensive polycistronism and antisense transcription in the Mammalian Hox clusters. *PLoS ONE* 2:e356.
43. Cohen SM, Brennecke J, Stark A (2006) Denoising feedback loops by thresholding–a new role for microRNAs. *Genes Dev* 20:2769–2772.
44. Bartel DP, Chen CZ (2004) Micromanagers of gene expression: The potentially widespread influence of metazoan microRNAs. *Nat Rev Genet* 5:396–400.
45. Hamburger V, Hamilton HL (1951) A series of normal stages in the development of the chick embryo. *J Morphol* 88:49–82.
46. Goff DJ, Tabin CJ (1997) Analysis of Hoxd-13 and Hoxd-11 misexpression in chick limb buds reveals that Hox genes affect both bone condensation and growth. *Development* 124:627–636.

DEVELOPMENTAL BIOLOGY